Three Dimensional Segmentation of the Heart Muscle in Real-Time 3D Echocardiographic Sequences Using Image Statistics

MM Nillesen[1], RGP Lopata[1], IH Gerrits[1], L Kapusta[2],
HJ Huisman[3], JM Thijssen[1], CL de Korte[1]

[1]Clinical Physics Laboratory, Department of Pediatrics,
[2]Children's Heart Centre, [3]Department of Radiology,
Radboud University Nijmegen Medical Centre, Nijmegen, the Netherlands

Abstract

A fully automated segmentation of the endocardial surface was developed by integrating spatio-temporal information of 3D ultrasound image sequences. 2D and 3D (adaptive) filtering was used to reduce speckle noise and optimize the distinction between blood and myocardium, while preserving sharpness of edges between various structures. Four different filters (2D Adaptive Mean, 2D and 3D Adaptive Mean Squares Filter and 2D Local Entropy) were tested. Filter quality was measured by comparing overlap percentages of histograms of manually segmented blood and myocardial regions. ROC curves of manually segmented blood regions were determined to compare effects of the different filters. A deformable contour algorithm was used, after automatic thresholding, to yield a closed contour of the endocardial border in each elevational plane. Each contour was optimized using contours of surrounding spatio-temporal planes as limiting condition to ensure spatio-temporal continuity.

1. Introduction

Finding the endocardial wall within echocardiographic images is an important preprocessing step for both volumetric studies and tissue characterization. Segmentation can be a helpful tool to visualize abnormalities in cardiac anatomy and to assess cardiac function and composition. Real-time 3D ultrasound images contain much information about the deformation cycle and the structure of the heart. 3D ultrasound is very suitable for imaging children as it is fast and non-invasive and, therefore, it might support clinical diagnosis of (congenital) heart disease at an early stage.

However, echocardiographic images are difficult to analyze. The images contain a high level of multiplicative speckle noise and the non-isotropic backscattering characteristics of the heart wall produce a low echo level at longitudinal incidence of the ultrasound with respect to fiber orientation. This causes a reduced distinction between blood and myocardium. Pediatric echocardiographic images are even harder to analyze, as image quality may be further reduced due to the smaller dimensions of the heart and relatively small intercostal spaces. Automatic segmentation of the heart wall is therefore a challenging scientific problem, and many strategies have been published in recent literature [1-4]. Segmentation methods that strongly rely on the shape and appearance of anatomical structures might fail to reveal cardiac abnormalities and, for this reason, are less suitable for echocardiographic images of children with a congenital heart disease. Deformable contour methods do not have this limitation. These methods use gradient information to steer the external forces to find edges, which will cause difficulties when applying such a technique to noisy ultrasound images. Therefore, some form of preprocessing of the ultrasound images might improve the performance of these techniques. Preprocessing should start with reducing the basic non-homogeneous characteristics of echographic images. In this paper, speckle reduction, based on image statistics, automatic thresholding and deformable models were combined to segment the heart muscle.

2. Methods

Echocardiographic image sequences of the left ventricle of four healthy children were obtained using thransthoracic short and long axis view. The 2D and 3D radiofrequency (RF) data were acquired using a Philips SONOS 7500 live 3D ultrasound system equipped with an RF-interface. An X4 matrix array transducer (2-4 MHz) and an S8 phased array transducer (3-8 MHz) were used to perform 3D and 2D imaging respectively. Data were transmitted to a workstation using a USB 2.0 interface.

A. Preprocessing

After the data was amplitude demodulated by using the Hilbert transform, spatial filtering was applied to denoise the images, while at the same time increasing the contrast

between blood and myocardium and preserving the sharpness of edges. Speckle characteristics are depth dependent due to beam diffraction and focusing, as well as due to attenuation, In particular, the lateral speckle size increases with depth [5,6]. This lateral speckle size in images obtained from a sector scanner can be homogenized in depth by processing the data along the scan lines, i.e., changing from a polar coordinate system into a rectangular matrix [7]. The data could thus be filtered using a sliding kernel with fixed size for all depths. The kernel size was expressed by a number of speckles rather than pixels, since speckles and not pixels should be considered as independent "grains of information" in echographic images of scattering media. Three adaptive filtering methods using 2D and 3D filtering kernels were applied and tested on the images: Adaptive Mean (AM) filtering (2D) and Adaptive Mean Squares (AMS) filtering (2D and 3D). The degree of smoothing was automatically steered by the homogeneity of the region the filter was operating on. Regions that contain edge are not homogeneous and therefore will be less smoothed than homogeneous regions, so this strategy guarantees preservation of the sharpness of the edges of various structures. These filters might optimize the discrimination between tissues such as blood, myocardium and pericardium. Besides adaptive filtering [8], local entropy [9] was used as a preprocessing step. Although the method itself is non-adaptive, this method is also based on the homogeneity (amount of information) in a region and contours are largely preserved.

B. Filter Quality

Two quality measures were developed to test whether the filters non-linearly adjusted the echographic gray-level information such that after filtering, the gray levels of blood and tissue did become more separated. Blood and myocardial regions were interactively segmented by an expert in the 2D axial-lateral plane for a set of images of each subject. The overlap percentages of the histograms from these two regions before and after filtering were used as a first quality measure. Histograms were normalized and then analyzed in the log(gray-level) domain. The difference in overlap percentages of blood and myocardium was tested using a Wilcoxon rank sum test over all datasets.

As a second measure for the quality of the different filtering method, the area under the ROC curve (AUC) was determined (ROCKIT) for the manually segmented blood regions. The blood region was then compared to tissue (myocardium, papillary muscles and pericardium), as this corresponds to the endocardial contour in the automatic thresholding method algorithm. Specificity and sensitivity were calculated for ROC analysis. To compare the difference in AUCs before and after filtering, a z-score was computed for each dataset separately, and t-test was performed over all datasets.

C. Automatic Thresholding

The Otsu method [10] was applied recursively to the data for finding the optimal threshold between blood and myocardium automatically. Thresholding was performed on the logarithm of the data because of the large spread in the case of the AM- and AMS filters. In case of the local entropy, filtered data were thresholded without the logarithmic compression because the histograms of the linearly encoded images were rather symmetric already. The optimal threshold was then used to generate a binary image in which blood is separated from the solid the tissues. Homomorphic filtering was applied to improve the result by removing spurious echoes. The resulting image was then used as the input for the deformable contour algorithm.

D. Deformable Contour

To find the endocardial contour, a deformable contour algorithm [11] including an inflating force [12] was applied to all elevational planes of the 3D volume. As the heart moves in a continuous way, continuity of the endocardial contours in spatial and temporal directions was assumed.

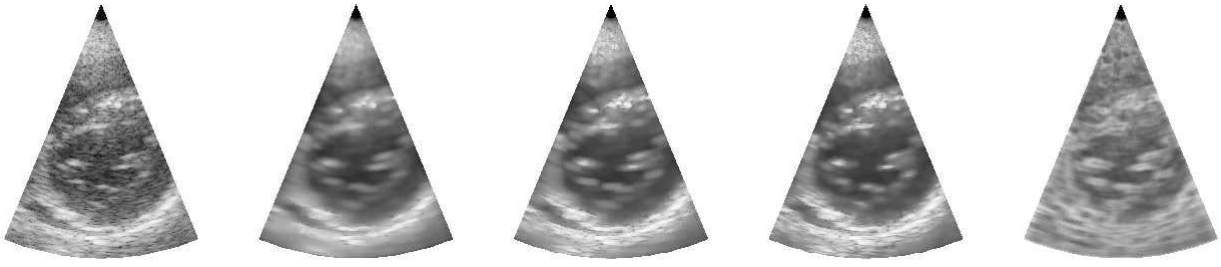

Figure 1 Example of the four filtering methods for a single plane of a 3D dataset. From left to right: unprocessed data, AM filter 2D, AMS filter 2D, AMS filter 3D and local entropy 2D.

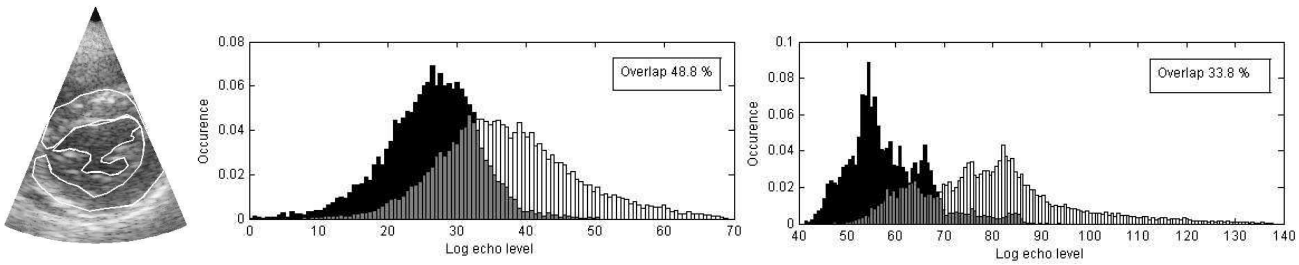

Figure 2. Manually segmented contours of blood and myocard regions unprocessed data *(left)*. Normalised histograms of blood and myocard before *(center*) and after *(right)* 2D AMS filtering .

Transforming this assumption to boundary conditions of the deformable contour algorithm, the contour in the current plane C(x, t) is optimized by using contours of adjacent planes in time and place as limiting condition. For spatial continuity C(x-1, t) is used as limiting condition. Temporal continuity is imposed by using C(x, t-1) to limit C(x,t). To initialize the algorithm, the first contour was computed in the systolic phase in the foremost plane of the 3D dataset, without any optimization in terms of continuity. For each frame, the endocardial contours obtained by the optimized deformable contour algorithm were combined to form the endocardial surface.

3. Results

The quality of the four different filters was examined for 16 datasets of the four children. In 10 of the datasets 3D data were contained. Figure 1 shows that the four filtering techniques resulted in a reduction of speckle noise and preservation of the sharpness of the edges. It can be seen that inhomogeneous regions, such as the pericardium, were almost unaffected by the adaptive filtering procedures, whereas the entropy method also smoothed these regions. The entropy method resulted in slight changes of the position of the edges.

Overlap percentages of the histograms of the manually segmented blood pool and myocardial region before and after filtering were computed for all 16 datasets. Figure 2 shows an example of manually drawn contours together with the histograms of these regions before and after filtering. In this case, the overlap percentage of blood and myocardial regions decreased from 48.8% before filtering to 33.8% after 2D AMS filtering. Table 1 lists mean and standard deviation of overlap percentages for all 3D datasets. All filter techniques showed a decrease in overlap percentage for all individual cases. A Wilcoxon rank sum test on the difference in overlap of histograms of blood and myocardium before and after filtering showed a significant decrease ($p < 0.01$).

Average values and standard deviations for the AUCs are denoted in Table 1, where a higher AUC indicates a higher accuracy. Both statistical tests on the difference in AUC showed that, compared to the AUCs of the unprocessed data, AUCs of the filtered data have increased significantly. However, mutual comparison of the four filters indicated that there is no significant difference in overlap percentages nor in AUCs. The 2D AMS filter, in combination with automatic thresholding, was chosen as preprocessing step for the deformable contour algorithm as this filter performed well on both overlap percentage and AUC tests.

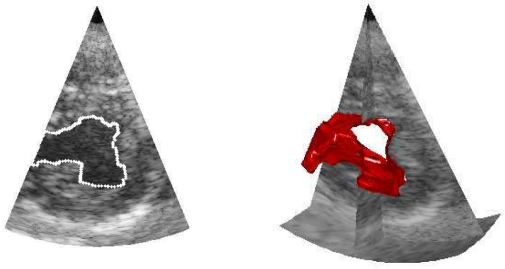

Figure 3. Optimized deformable contour *(left)* and resulting endocardial surface *(right)*.

The deformable contour algorithm was applied to a 3D dataset acquired over a full heart cycle to find the endocardial surface. Visually plausible contours were obtained for all elevational planes. Using 4D information by imposing spatial and temporal continuity for contours of the separate planes, better segmentation of the ventricle was obtained rather than by using information of each plane separately. An example of one particular elevational plane of the heart cycle and the complete endocardial surface is shown in Fig. 3. The endocardial surface shows coherence between the contours of adjacent planes, following the assumption of temporal and spatial continuity of the heart movement used by the deformable contour algorithm. Due to possible anatomical abnormalities of the heart in children, no smoothing of the endocardial surface was performed as this might have blurred anatomical details.

Table 1. Overview of mean and standard deviation of histogram overlap percentages and AUC of ROCs for unprocessed data and different filtering methods

	Gray level histogram		ROC analysis	
Filter method	Mean overlap % n = 10	Standard deviation of overlap %	Mean AUC % n = 10	Standard deviation of the mean AUC %
Unprocessed data	44.2	3.7	88.48	3.1
AM filter	29.0	6.4	93.41	2.8
AMS filter	28.6	6.0	94.04	2.7
AMS3D filter	28.5	5.4	94.19	2.9
Entropy	29.1	6.1	94.11	2.9

4. Discussion and Conclusion

A three-dimensional segmentation method of the endocardial surface was described. The preliminary results of the study indicate the potential of the combination of adaptive filtering using image statistics and deformable contours. The method is fully automated, no user interaction is required, except from the choice of the initial plane the deformable contour algorithm is started from. In clinical practice, this initial starting plane can be automatically chosen if 3D volumes are acquired in a standard way. Selection of the proper starting frame in time can be done using the ECG. The ECG can also be used to improve the segmentation algorithm by integrating information related to the phase within the cardiac cycle. Adaptive filtering also improves the distinction between myocardium and pericardium and, therefore, can also be used as a preprocessing step for segmenting the pericardium. Although the method is used to perform three-dimensional segmentation, the method has to be optimized by using 3D deformable surfaces to integrate temporal and spatial information more strongly. As the myocardium is an inhomogeneous structure and because only a fraction of the myocardial muscle fibers is perpendicular to the ultrasound beam, part of the myocardium has very low echogenicity and is hard to distinguish from (electronic) background noise. This may cause problems in the segmentation process if prior knowledge about the anatomy would completely discarded.

Acknowledgements

This work is supported by the Dutch Technology Foundation (STW), project NKG 6466.

References

[1] Angelini ED, Homma S, Pearson G, Holmes JW, Laine AF. Segmentation of real-time three-dimensional ultrasound for quantification of ventricular function: a clinical study on right and left ventricles. Ultrasound Med Biol 2005 Sep;31(9):1143-58.

[2] Bosch JG, Mitchell SC, Lelieveldt BP, Nijland F, Kamp O, Sonka M, et al. Automatic segmentation of echocardiographic sequences by active appearance motion models. IEEE Trans Med Imaging 2002 Nov;21(11):1374-83.

[3] Dydenko I, Friboulet D, Gorce JM, D'hooge J, Bijnens B, Magnin IE. Towards ultrasound cardiac image segmentation based on the radiofrequency signal. Med Image Anal 2003 Sep;7(3):353-67.

[4] Gerard O, Billon AC, Rouet JM, Jacob M, Fradkin M, Allouche C. Efficient model-based quantification of left ventricular function in 3-D echocardiography. IEEE Trans Med Imaging 2002 Sep;21(9):1059-68.

[5] Oosterveld BJ, Thijssen JM, Verhoef WA. Texture of B-mode echograms: 3-D simulations and experiments of the effects of diffraction and scatterer density. Ultrason Imaging 1985 Apr;7(2):142-60.

[6] Thijssen JM, Oosterveld BJ. Performance of echographic equipment and potentials for tissue characterization. Berlin: Springer; 1987 p. 455-68.

[7] Valckx FM, Thijssen JM, van Geemen AJ, Rotteveel JJ, Mullaart R. Calibrated parametric medical ultrasound imaging. Ultrason Imaging 2000 Jan;22(1):57-72.

[8] Bamber JC, Daft C. Adaptive filtering for reduction of speckle in ultrasonic pulse-echo images. Ultrasonics 1986 Jan;24(1):41-4.

[9] Kapur JN, Sahoo PK, Wong AKC. A New Method for Gray-Level Picture Thresholding Using the Entropy of the Histogram. Computer Vision Graphics and Image Processing 1985;29(3):273-85.

[10] Otsu N. Threshold Selection Method from Gray-Level Histograms. Ieee Transactions on Systems Man and Cybernetics 1979;9(1):62-6.

[11] Kass M, Witkin A, Terzopoulos D. Snakes - Active Contour Models. International Journal of Computer Vision 1987;1(4):321-31.

[12] Cohen LD. On Active Contour Models and Balloons. Cvgip-Image Understanding 1991 Mar;53(2):211-8.

Address for correspondence
Maartje M. Nillesen
P.O. Box 9101, 6500 HB, Nijmegen, the Netherlands.
m.m.nillesen@cukz.umcn.nl